

K&C Science Report – Phase 2

A wall-to-wall PALSAR mosaic of Africa

Gianfranco De Grandi and Alexandre Bouvet
European Commission, DG Joint Research Center, TP 440, 21020 Ispra (VA), Italy. frank.de-grandi@jrc.it

Richard Lucas
University of Wales at Aberystwyth

Masanobu Shimada
Japan Aerospace Exploration Agency (JAXA), Tsukuba, Japan.

Stefano Monaco
SARMAP, Cascine di Barico, Switzerland.

Ake Rosenqvist
soloEO, TTT Mid-Tower #607, Kachidoki 6-3-2, Chuo-ku, Tokyo 104-0054, Japan.

Abstract— In the framework of the JAXA Kyoto and Carbon (K&C) project, blanket and systematic observations were acquired by the PALSAR synthetic aperture radar (SAR) in FBD dual-pol mode over those ecosystems of the world, which are of importance for climate change studies, carbon science, environment conservation and related environmental treaties. Starting from these observations, the role of JRC was to assemble a wide area and high spatial resolution (order of 100 m) mosaic of PALSAR images covering the whole African. The mosaic is a dual-band (HH-HV) data set geo-referenced and terrain corrected (by a SRTM DEM) to a latitude-longitude coordinate system with pixel spacing of $8.333 \cdot 10^{-3}$ degrees. The main computational and radar science issues, which had to be taken into account to arrive from raw data at seamless imagery with good radiometric and geometric accuracy, are summarized.

Index Terms—ALOS PALSAR, K&C Initiative, Africa, mosaic.

I. INTRODUCTION

The thematic information relevant to K&C has to satisfy criteria of spatial consistency over very large areas (regional / continental scale) and, at the same time, of high spatial resolution (order of 100 m). To the purpose, large mosaics composed of radar images acquired along hundreds of orbits need to be assembled.

A collaborative effort among several partners of the K&C project has led to the generation of these data sets. We report here on the experience gained in one such collaborative effort, aimed at developing a wide area PALSAR mosaic over the whole African continent. A snapshot of the mosaic is shown in Figure 1. The mosaic is a dual-band (HH-HV) data set

referenced to a latitude-longitude coordinate system with pixel spacing of 8.333 degrees (roughly 100 m at the equator).

The compilation of a large number of SAR images into a synoptic view of a wide planetary surface for lending support to studies of global geo-physical processes is certainly not a new deed. Previous works have paved the way: the Central Africa mosaic of C-band ERS-1 [1], and the mosaics over the whole tropical and Boreal forest eco-zones of the world, composed of L-band JERS-1 imagery supplied by the JAXA [2][3][4]. These projects were indeed the precursors of K&C, and did set the stage for building the technical know-how which is required for the development and the analysis of wide-area high resolution radar mosaics. However, the K&C development signals one step higher in the scale of performance - hence complexity - with respect to its precursors, due to: i) the availability of the cross-polarized backscattered power (HV) together with a co-polarized return (HH); ii) the availability of a high-quality digital elevation model with comparable spatial resolution over the whole mosaic's extent; iii) a new type of SAR image product developed by JAXA, based on focusing the raw data along extended segments of the sensor's orbit, and thus more convenient for large area coverage; iv) improved sensor's performance with respect to radiometric (stability) and geometric accuracy; v) optimized acquisition plan which guarantees full coverage of the area of interest (continent) in the shortest time compatible with the sensor's orbital cycle (2 months in the case of Africa).

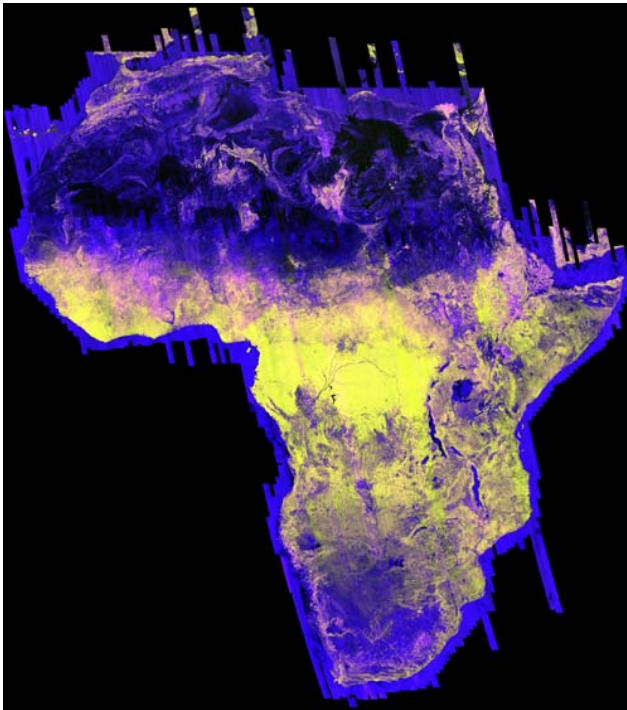


Figure 1. The K&C continental-scale Africa mosaic. The mosaic was assembled from PAISAR fine beam dual pol (FBD) images (HH band shown), which were geocoded into a geographic unprojected (latitude, longitude) coordinate system with a pixel spacing of 0.8333 millidegree (roughly 100 m at the equator).

These two last aspects are of paramount importance for the generation of seamless mosaics, which in turn is a precondition for the successful thematic exploitation of the data sets. The availability of the cross-polarized channel is very important, for instance, in thematic applications related to forest mapping, since cross-polarization arises from volume scattering, and therefore it is proportional to the woody biomass in the forest crown, to the trunk biomass through double bounce scattering, and less sensitive to direct ground contribution. The availability of a high quality digital elevation model paves the way to the utilization of precision geo-coding, of radiometric corrections for effects induced by topography, and of terrain morphology measures as additional training sets in a classification procedure.

This report will give an account of the state of the art concerning the generation of the K&C Africa mosaic, an assessment of the data set quality, and preliminary observations which document the richness in information content, and the potential for future thematic applications. In section II an overview is given of the bespoke processing chain that was designed for the generation of the mosaic, and the main processing issues which arose in the implementation phase are discussed. Conclusions and recommendations for this paper are provided in Section V.

A. The mosaic processing chain

The K&C PALSAR raw data were focused on a routine basis by JAXA during the fall 2007, using a proprietary SAR processor (SigmaSAR). The processor generates path images in slant range, amplitude data at two polarisations (HH, HV), with 16 looks in azimuth and 2 looks in range, a pixel spacing of 37.47 m in range, 19.2 m in azimuth, and image size corresponding, in ground range, to approximately 70 km in range, and up to 2000-3000 km in cross-range.

Features of the K&C path data sets (i.e. data volume, non-linear geometry and radiometric anomalies) call for the development of bespoke processing chains for the assemblage of wide area mosaics with suitable geometric and radiometric quality.

To the purpose a number of algorithms for the geometric and radiometric revision and the path images assembly were studied and implemented. This effort was conducted in collaboration with a Swiss company (SARMAP SA).

Functionalities implemented in the K&C Africa mosaicking software include:

- House keeping routines to handle the ingestion and the file structure of the JAXA path image data sets.
- Adaptive calibration revision of the original slant range data sets. This module automatically checks for the presence of radiometric anomalies and calibrates accordingly the data (see section II.B).
- Extraction of subsets corresponding to the geographical extent of each projected strip image from a continent-wide digital elevation model (DEM) over Africa. The DEM is derived from Shuttle Radar Topographic Mission (SRTM) data [5].
- Geo-coding into a geographic reference coordinate system (e.g. un-projected latitude-longitude) using the solution of the range-Doppler equations. This step also produces auxiliary data holding the effective local incidence angles for each pixel of the backscatter amplitude image (see Section II.5)
- Compression / decompression of the geo-coded imagery to optimize data volume and processing time.
- Assemblage of the geo-coded strips within a geographic bounding box. The module uses an inter-strips amplitude blending algorithm to avoid edge effects.
- Mosaic's radiometric revision to correct for seasonality effects and residual calibration errors, based on the estimation of backscatter differences along overlapping borders of neighboring strips (see section II.4).

The bespoke modules are interfaced through a batch processor to the underpinning functions (e.g. geo-coding) provided by the commercially available software SARscape by SARMAP SA [6]. In this way large batch of data can be processed in background, while operator's intervention is limited to some critical steps, like the mosaic's calibration revision. Indeed

optimization of processing resources (memory, disk space) and processing time was one of the challenges posed by the construction of a high resolution continental scale data set. In the following we will expand on the main issues that had to be resolved in the design and implementation of the processing chain in connection with the characteristics of the Africa mosaic's radar imagery.

B. Radiometric revision of path slant range images

Insight into the radiometric fidelity of K&C path data sets can be gained considering average slant range profiles. The profiles are computed by selecting areas which are as homogeneous as possible regarding the illuminated target from near to far range.

An example is shown in Figure 2. The related data set is KC_004-13611N17S10FBDSL1 (according to JAXA file naming convention) at HH polarization. The range profile (white line in the graph, the red line indicates the corrected profile after the revision) was estimated using a block of 512 lines (amplitude slant range data) bracketing an area of homogeneous dense tropical forest extending from near to far range. Two features are strikingly evident by inspection of the graph: a linear negative trend of the amplitude signal from near to far range, and an abrupt, almost complete loss of power at the end of the swath. Quantitatively the power ratio between near and far range is roughly -2 dB. This amount of power loss cannot be justified either by the dependence on ground scattering area, nor by dependence of the radar cross section on incidence angle. In the first case, assuming that data provided by JAXA are proportional to power per unit area in slant range, the power ratio for the range of incidence angles in this data set should be roughly -0.04 dB. In the second case, wave scattering modelling of the dense tropical forest indicates that the power ratio at HH due to dependence of the radar cross section on incidence angle should be of the order of -0.13 dB. Similar considerations apply for areas dominated by surface scattering (e.g. bare soil, water).

This analysis suggests that two radiometric anomalies affect the data and should be taken into consideration in a revision process: complete loss of signal at image margin in range direction, and linear signal drop from near to far range within the segment with a valid signal.

However, the problem is compounded by the fact that such anomalies are not observed systematically and consistently throughout the data sets used in the compilation of the mosaics. The abrupt power drop sometime happens at far range, sometime at near range, or even at both far and near range (presumably as a function of latitude in the geographic position of the strip image). The linear negative trend in range is not consistent in terms of rate of decay throughout data sets, and within the same set depends on average backscatter. Moreover in many cases the anomaly is not present at all.

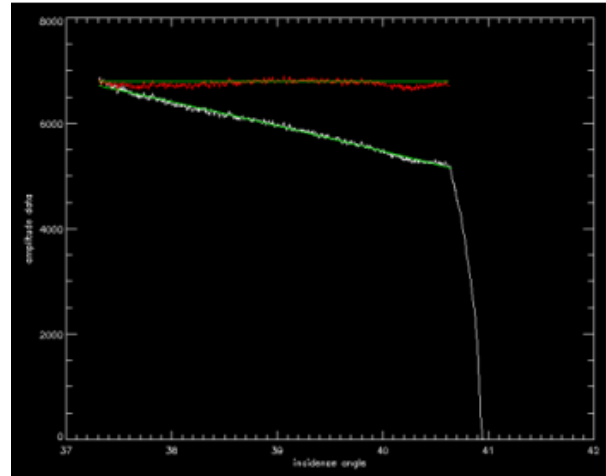


Figure 2. Range profile as a function of incidence angle showing the power loss at the end of swath and the linear negative trend within the swath (white line in graph). The red line shows the corrected profile after the adaptive calibration procedure.

This scenario strongly suggests that the radiometric revision process of the K&C strip data cannot be based on theoretical global correction functions, even if parameterized by free variables, but must per force rely on an adaptive algorithm driven by local estimation of the radiometric trends and anomalies.

The basic assumptions underlying the algorithm are:

1) The negative linear trend in range is system induced by a multiplicative gain function:

$$g(r) = g(0) + m \times r \quad (1)$$

where r is the range coordinate (pixel index in the column direction of the slant range data), m and $g(0)$ are the parameters of the linear fit.

This function can be estimated by averaged range profiles in homogeneous regions. The range profile is fitted linearly and a correction multiplicative function defined as:

$$c(r) = 1 - \frac{m \times r}{g(0)} \quad (2)$$

2) In the same data set the rate of decay of the linear trend (if present) can be characterized by two functions $g_1(r), g_2(r)$ associated (in loose sense) to areas dominated by volume scattering and surface scattering. In turn, these areas, given that the thematic content of interest comprises mainly forest, woodland, bare soil, or soil with low vegetation, can be identified by segmenting the range of backscatter values in the data set into two classes: low backscatter and high backscatter. Specific threshold values for identifying the two classes must be chosen as a function of the polarization. The two-class segments are disjoint. Therefore the region in-between is

characterized by a continuous functional $F(g_1, g_2)$ of the two functions g_1 and g_2 .

In a nutshell, the algorithm is composed of three steps:

i) Detection and removal of the power drop at the data set margins. ii) Estimation of the linear power trend in range by a search of the most homogeneous block, and for two backscatter classes (a proxy for volume and surface scattering). iii) Application of an inverse gain function based on the estimated trends.

C. Radiometric inter-strip balancing

Analysis of the mosaicked image compiled from the geo-coded and range calibrated strips reveals the presence of inter-strips radiometric discontinuities. In particular, some strips present remarkable differences in backscatter values (order of 2 dB) with respect to the adjacent ones (see Fig. 3). The origin of this effect can be traced back to seasonality and weather conditions (mostly the effect of soil moisture. Indeed, to assure spatial continuity, part of the 2007 acquisitions corresponding to the dry-season at tropical Central Africa had to be complemented with acquisitions during the wet-season. This difference in time can account for difference in radar reflectivity due to evolution in the target's properties (e.g. change in vegetation cover, change in soil and vegetation moisture). In the overlap area between two adjacent strips the same target on the ground is seen by the radar with a different incident angle (far and near range). Assuming a cosine law for the radar cross section dependence on incidence angle, the difference in backscatter due to near-far range incidence angle difference is roughly 0.78 dB, hence of the order of PALSAR radiometric accuracy. However, this figure in dB corresponds to a power DN ratio of 1.196, which would still give visible edge effects in the imagery. Other minor inter-strip unbalancing is produced by residual errors in range calibration.

The first approximation mosaic needs therefore to be corrected to arrive at a more radiometrically homogeneous version, which could be suitable for successive automatic interpretation, or for the estimation of bio-physical parameters, such as forest biomass. This correction is achieved by an inter-strip balancing algorithm which relies on information derived by along-track profiles of the backscatter values estimated within the area of overlap between one strip and all the surrounding ones. Since the radiometric discrepancies depend on the position within the strip (land cover and conditions), it is not possible to define a global strip-wise gain factor. Therefore, a gain function is defined for each strip which depends linearly on the column coordinate (approximate range direction) of the strip frame, and it is a piece-wise linear approximation along the line coordinate (along track direction) of the ratio between the strip border profile and the corresponding profiles of the neighboring strips. A strip frame is defined as the area where there are available values in the geo-coded image.

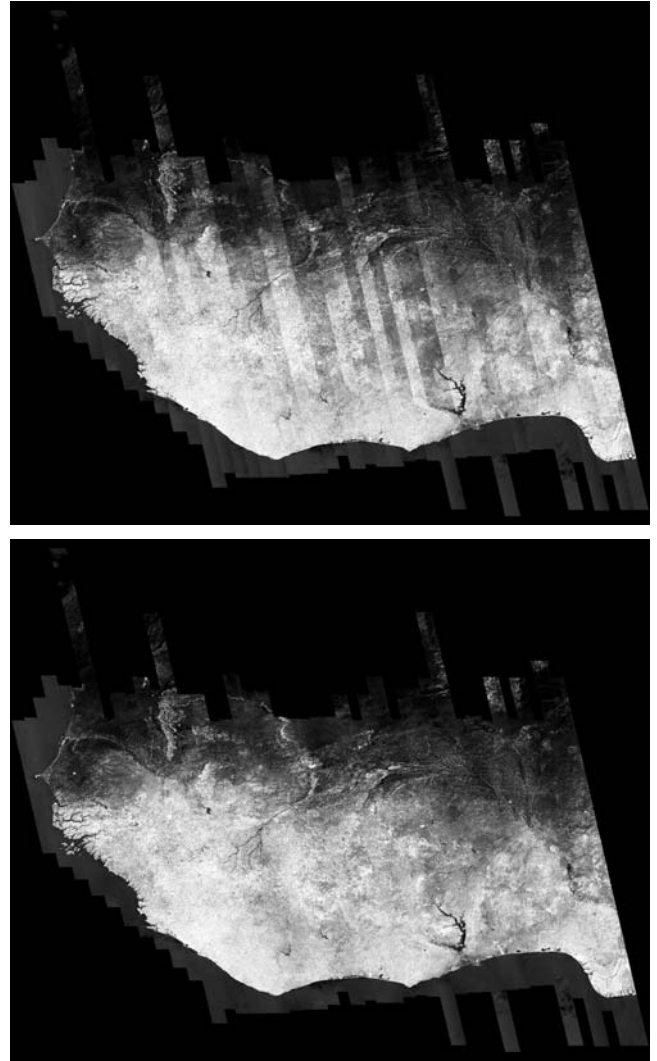


Figure 3. The West Africa part of the mosaic. Relevant radiometric differences (order of 2dB) are clearly visible between adjacent strips in the original not corrected mosaic (top frame). The mosaic after the radiometric balancing based on inter-strip discrepancy measures is shown in the bottom frame.

Thus, calling $P_k^{\text{left}}(i)$ and $P_k^{\text{right}}(i)$ estimates of the mean DN values along the left and right borders at position i along track of strip k , and $P_{k-1}^{\text{right}}(i)$, $P_{k+1}^{\text{left}}(i)$ estimates of the corresponding profiles of adjacent strips at left and right of strip k , we define discrepancy measures as:

$$D^{\text{left}}(i) = \frac{P_{k-1}^{\text{right}}(i)}{P_k^{\text{left}}(i)} \quad (3)$$

$$D^{\text{right}}(i) = \frac{P_{k+1}^{\text{left}}(i)}{P_k^{\text{right}}(i)}$$

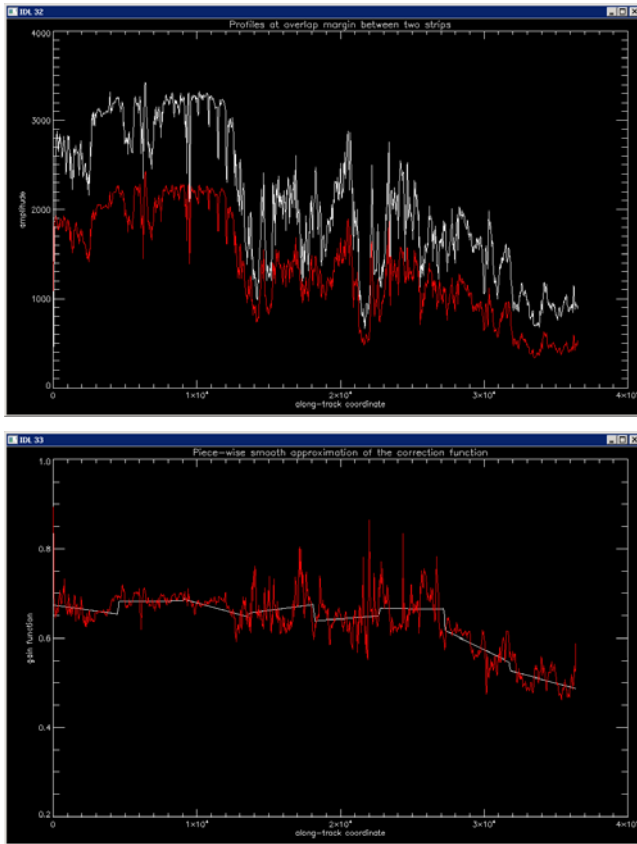


Figure 4. Profiles in the along-track direction of mean DN values of the overlap area at the margin between two adjacent strips (upper graph). The radiometric differences are not constant along track, a fact that suggests the use of a variable gain function. This gain function is estimated by a piece-wise linear fitting of a smoothed version of the ratio between the two along-track profiles (lower graph).

An example of the discrepancy measure and the related gain function is shown in Fig. 4.

These discrepancy measures form the basis for the mosaic correction algorithm.

As a first step, the measures $D(i)$ are used to locate the strips that are affected by large radiometric discrepancies. To the purpose, the mode of the distribution (density function) of D^{left} and D^{right} is computed. This figure of maximum discrepancy between adjacent strips is further screened by an operator, and used to flag the strips as anomalous ones. An automatic detection of anomalous strips is difficult, because the eventual occurrence in the same mosaic of strips with higher and lower than normal DN values renders the discrepancy measures ambiguous.

Once the anomalous strips have been flagged, the algorithm proceeds according to the following principle. Gain functions are defined for the anomalous strips using $D^{left}(i)$ and $D^{right}(i)$ measures with respect to normal adjacent strips. In

the event that a second anomalous strip is present near the first one, then the gain function is computed from the only available measure (left or right) and assumed constant in range. This approach limits the possible number of consecutive anomalous strips to two. Indeed, this condition was satisfied in the processing of the whole Africa mosaic.

These gain functions balance the anomalous strips' radiometry to match the ones of the adjacent strips. Next, the residual trends in range calibration and other minor inter-strip unbalances are corrected by sharing the correction weight between the neighboring strips (moving the trend half way up and half way down). In this way the danger of error propagation is avoided.

More in detail, the mosaic balancing algorithm consists of the following steps:

- 1) Construction of a data structure that holds information on the neighbors of each strip. This is achieved starting from a strip layout map which is generated by the mosaicking procedure, and where each strip position in the mosaic's canvas is assigned a unique identifier.

- 2) Computation for each geocoded strip k of the profiles P_k and discrepancy measures D_k . Since one strip can have several neighbors at left or right, a data structure ID is also generated that keeps track of who is the neighbor for each value of the profile, and how the line coordinate of the two strips are related. Thus: $P_k(i) \Leftrightarrow ID(i)$. The structure ID is used when a discrepancy measure must be updated because an anomalous strip was corrected by a gain function. This is the only step that requires ingestion of the actual strip data sets.

- 3) Discrepancies analysis and choice of the anomalous strips by an interactive procedure.

- 4) Generate gain functions for the correction of anomalous strips. As explained above, these functions are derived from the discrepancy measures relative to adjacent normal strips. These gain functions are computed by a piece-wise linear fitting of the D_k functions. In fact, the D_k functions, being ratios of two samples from speckle noise, would introduce artifacts if used as multiplicative factors of the strip amplitude data. The D_k functions are first low-pass filtered and down-sampled by a factor of 64 to obtain a slow-varying trend. This trend function is then split iteratively into an increasing number of consecutive segments. At each step of the iteration the segments are linearly fitted, and the global rms differences computed. The procedure is stopped when the rms differences between two steps increase or after a maximum number of divisions. The piece-wise linear trend is then up-sampled to the original resolution by spline interpolation. The gain functions for anomalous strips are stored as vectors in files to be used later by the mosaicking procedure in the compilation of the second approximation revised mosaic.

- 5) Upgrade the profiles P_k of the anomalous strips with respect to the gain functions defined in the preceding step. Re-

compute the discrepancy measures D_k which have been affected by a change of the P_k .

6) Generate gain functions for all strips from the D_k functions as:

$$g_k^{left}(i) = \frac{1}{2} LININTERP(D_k^{left}(i)) + \frac{1}{2} \quad (4)$$

$$g_k^{right}(i) = \frac{1}{2} LININTERP(D_k^{right}(i)) + \frac{1}{2}$$

The gain function used by the mosaicking procedure for the mosaic balancing will finally be:

$$g_k(i, j) = \frac{g_k^{right}(i) - g_k^{left}(i)}{\Delta j} j + g_k^{left}(i) \quad (5)$$

The results obtained by the strip balancing algorithms are documented in Fig 5.

D. Geocoding

Terrain geocoding of the slant range path data sets is performed using a module of the SARscape software [6]. A continent-wide digital elevation model (DEM) of Africa derived from the Shuttle Radar Topography Mission (SRTM) data [5] is adopted. This DEM is provided in a geographic projection (Lat/Lon coordinates) using the WGS-84 horizontal datum, with a pixel size of 3 arc seconds (i.e. 0.8333 millidegrees, approximately 90m at the equator). The geocoded PALSAR imagery of the Africa mosaic are generated in the same projection and spatial resolution of the DEM. This choice assures the best geometric and radiometric accuracy (see also section II.6). Moreover past experience with thematic applications based on GRFM data sets indicate that the adopted pixel spacing is suitable for regional scale vegetation mapping studies. Higher spatial resolution is only needed for particular tasks, such as selective logging monitoring, which, on the other hands, are conducted at local scale.

SARscape geocoding is based on the classical range-Doppler approach. Note that this is the only appropriate way to obtain precision geocoding of SAR data. In fact, SAR systems cause nonlinear distortions (in particular in the presence of topography), and thus they cannot be corrected using polynomials as in the case of optical images, where (in the case of flat Earth) an affine transformation is sufficient to convert it into a cartographic reference system.

Mapping from the slant range SAR geometry into a cartographic projection is obtained by considering the sensor's and the image focusing parameters. Therefore the range-Doppler approach calls for the solution of the following relations:

$$\bar{R}_s = \bar{S} - \bar{P} \quad (6)$$

$$f_D = \frac{2(\bar{v}_p - \bar{v}_s) \bullet \bar{R}_s}{\lambda |R_s|} \quad (7)$$

where \bar{S} and \bar{P} are the sensor and target position vectors, $\bar{v}_p - \bar{v}_s$ is the velocity of the target relative to the sensor, and λ is the wavelength of the carrier.

The geocoding is implemented by a backward solution of the range-Doppler equations. Starting from each point of the DEM reference system, the corresponding point in the slant range radar geometry is found using the range Doppler equations. Elements from the SAR geometry frame are then re-sampled into the earth projection (DEM) coordinate system.

Notice that the JAXA K&C path products are not processed at zero-Doppler. Therefore in the solution of (7) the proper value of the Doppler centroid had to be used. These values are supplied by JAXA in an auxiliary file.

Sources of geometric errors in SAR geocoding propagate from satellite orbit, range time, Doppler frequency and DEM accuracies [7]. In our case, assessment of the geocoding accuracy was conducted a-posteriori by establishing common features with the same DEM used in the geocoding procedure. It is therefore a relative accuracy measure. Difference vectors between control points in the SAR image and in the reference DEM image were defined by visual inspection. The maximum difference vector magnitude was found to be one pixel.

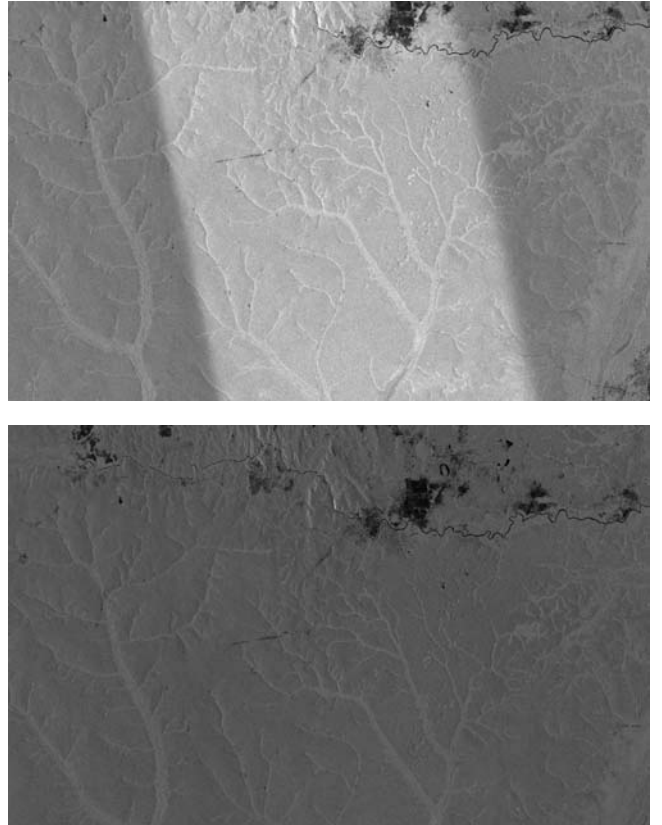


Figure 5. The result of the strip balancing algorithm when applied to a set of strips with one radiometric anomaly viz. higher backscattering coefficient possibly due to vegetation moisture change (see section III for related analysis).

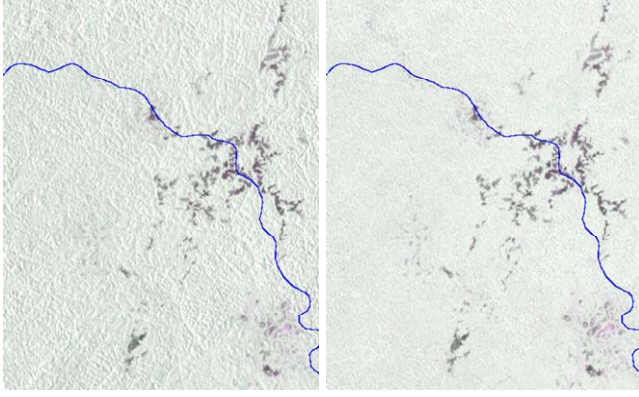


Figure 6. Effect of the radiometric correction for topographic effects portrayed in a scene at the border between DRC and Gabon, featuring moderate relief. The images are color-composite of HH-HV-HH amplitude data.

E. Radiometric correction for topographic effects

SAR radiometry is affected by topography due to changes of the ground scattering area, and to changes of the local incidence angle, which in turn has an impact on the backscattering properties of the targets. Correction of these effects is important to make the data set suitable for automatic classification [8] [9]. On the other hand, application of these corrections tend to smooth features related to terrain morphology, and therefore renders the data set less amenable to visual interpretation by the expert, at least for certain thematic applications. Therefore in our implementation we decided to apply radiometric normalizations for topography a-posteriori in a second instalment of the mosaics.

The normalization entails two corrections accounting for the effective scattering area, and the radar cross-section dependence on local incidence angle.

The effective ground scattering area A_{slope} is obtained by projecting the pixel area to the slope plane:

$$A_{slope} = \frac{r_d r_s}{\sin \theta_{loc}}$$

where θ_{loc} is the SAR local incidence angle, i.e the angle between the incident electromagnetic wave vector \vec{d} and the normal at the terrain surface \vec{n} .

In our case, \vec{n} is directly derived from the DEM at each pixel (x,y) by calculating the cross-product of the two three-dimensional vectors formed by the adjacent pixels in longitude and latitude respectively:

$$\vec{n} = \vec{v}_1 \wedge \vec{v}_2$$

These two vectors are given by:

$$\vec{v}_1 = \begin{pmatrix} 2 \cdot p_m \\ 0 \\ H_{x+1,y} - H_{x-1,y} \end{pmatrix} \text{ and } \vec{v}_2 = \begin{pmatrix} 0 \\ 2 \cdot p_m \\ H_{x,y-1} - H_{x,y+1} \end{pmatrix}$$

where p_m represents the pixel size in meters, and $H_{x,y}$ the altitude of the terrain at pixel (x,y) as given by the DEM.

The correction factor for the effective scattering area is finally:

$$C_{area} = \frac{\sin \theta_{loc}}{\sin \theta}$$

where θ is the nominal incidence angle for flat terrain.

The effect of incidence angle on the backscattering coefficient depends on the nature of the target as well as on the polarization. Two possible avenues can be taken for the correction of these effects: a) postpone the correction to the classification phase, given that a-priori information on the target type at the scale of the whole mosaic will be available from an auxiliary data sets (e.g. MODerate resolution Imaging Spectrometer (MODIS) optical data); b) tailor the correction to one specific thematic application, accepting to be sub-optimal for a general land cover mapping task. In view of our applications of interest (tropical forest and woodlands mapping) we decided to correct for the case of vegetation (dominated by volume scattering).

The angular dependence of forest backscatter is quite well represented by a cosine function, which accounts for the modified path length of the wave into the canopy [10]. Therefore the related correction factor is:

$$C_{angle} = \frac{\cos \theta}{\cos \theta_{loc}}$$

The backscatter coefficient corrected for the overall effect of topography is:

$$\sigma^0_{corr} (\text{dB}) = 20 \text{Log}_{10} (\text{DN}) + 10 \text{Log}_{10} \left(\frac{\tan \theta_{loc}}{\tan \theta} \right) - 83 \text{dB}$$

The efficacy of the topographic corrections is documented by the following cases.

Figure 6 shows the effect of the topographic correction on the images, for a small subset of the mosaic at the border between Congo and Gabon. The non-forest areas are more visible in the corrected image, when the backscatter variation due to relief is removed.

III. CONCLUSION

Using ALOS PALSAR L-band HH and HV strip data acquired in 2007, a mosaic of the African continent was generated at 100 m spatial resolution. A range of pre-processing routines (radiometric calibration, geocoding, incidence angle and topographic correction) were implemented to facilitate combining the strip data into the mosaic. However, the backscatter (particularly at HH polarisation) was enhanced in some strips, with this attributed to increased soil moisture at the time of the ALOS PALSAR data acquisition. A number of potential applications for the mosaic can be found in [11], including mapping of mangroves,

plantations, secondary forests and the boundary between savannas and forests. Comparison with the JERS-1 SAR mosaics also suggests significant potential for detecting deforestation. Plans for the future include the production at the JRC of a woodlands biomass map and of a land cover map of Africa using this mosaic. Both products will be useful to refine estimations of carbon stocks in Africa.

ACKNOWLEDGEMENTS

This work has been undertaken within the framework of the JAXA Kyoto & Carbon Initiative. ALOS PALSAR data have been provided by JAXA EORC.

REFERENCES

- [1] G.F. De Grandi, J.P. Malingreau, M. Leysen, "The ERS-1 Central Africa Mosaic: A New Perspective in Radar Remote Sensing for the Global Monitoring of Vegetation", *IEEE Trans. on Geosci. Remote Sensing*, vol. 37, no. 3, pp. 1730-1746, May 1999.
- [2] G.F. De Grandi, P. Mayaux, Y. Rauste, A. Rosenqvist, M. Simard and S. Saatchi, "The Global Rain Forest Mapping Project JERS-1 Radar Mosaic of Tropical Africa: Development and Product Characterization Aspects", *IEEE Trans. on Geoscience and Remote Sensing*, 38(5), 2218-2233, 2000.
- [3] A. Rosenqvist, M. Shimada, B. Chapman, K. McDonald, G. De Grandi, H. Jonsson, C. Williams, Y. Rauste, M. Nilsson, D. Sango, M. Matsumoto, "An overview of the JERS-1 SAR Global Boreal Forest Mapping (GBFM) project", *Proc. of the IEEE Geoscience and Remote Sensing Symposium, IGARSS '04, Volume: 2, 2004*, Page(s): 1033 - 1036.
- [4] Paul Siqueira, Scott Hensley, Scott Shaffer, Laura Hess, Greg McGarragh, Bruce Chapman, and Anthony Freeman, "A Continental-Scale Mosaic of the Amazon Basin Using JERS-1 SAR", *IEEE transactions on Geoscience and Remote Sensing*, vol. 38, no. 6, Nov. 2000.
- [5] Jarvis, A., H.I. Reuter, A. Nelson, E. Guevara, 2008, Hole-filled SRTM for the globe Version 4, available from the CGIAR-CSI SRTM 90m Database: <http://srtm.csi.cgiar.org>.
- [6] "SARscape short technical description", sarmap SA, available at: <http://www.sarmap.ch/pdf/SARscapeTechnical.pdf>
- [7] Schreier, G.; Raggam, J.; Strobl, D., "Parameters For Geometric Fidelity Of Geocoded Sar Products", *Proc. IEEE Geoscience and Remote Sensing Symposium, IGARSS '90*, pp. 305 - 308, 1990.
- [8] J.J. Van Zyl, "The effect of topography on radar scattering from vegetated areas", *IEEE Transactions on Geoscience and Remote Sensing*, vol. 31, no. 1, pp. 153-160, 1993.
- [9] F. Holecz, U. Wegmüller, E. Rignot, and Y. Wang, "Observed radar backscatter from forested areas with terrain variations", *Proceedings IEEE International Geoscience and Remote Sensing Symposium, Firenze*, vol. 1, pp. 613-615, 1995.
- [10] T. Castel, A. Beaudoin, N. Stach, N. Stussi, T. Le Toan, and P. Durand, "Sensitivity of space-borne SAR data to forest parameters over sloping terrain. Theory and experiment," *International Journal of Remote Sensing*, vol. 22, pp. 2351-2376, 2001.
- [11] G.F. De Grandi, A. Bouvet, R. Lucas, "Wide area K&C PALSAR mosaics : Processing issues and first thematic results", *EUSAR 2010 proceedings*



Gianfranco D. De Grandi received the Doctorate degree in physics engineering (with honors) from the Politecnico Milano, Milan, Italy, in 1973. Since 1977, he has been with the European Commission Directorate General Joint Research Center, Ispra, Italy, where he has performed research in signal processing for gamma ray spectroscopy, data communications, and radar remote sensing. In 1985, he was a Visiting Scientist with Bell Communications Research, Morristown, NJ, where he participated in the design of Metrocore, which is one of the first research projects for gigabit-rate metropolitan-area networks. From 1997 to

2001, he was an Assistant Professor with the Faculté de Géomatique, Université Laval, Quebec, QC, Canada. He is a Principal Investigator of the Japan Aerospace Exploration Agency (JAXA) Global Boreal Forest-Mapping Project, the JAXA ALOS Research Program, and the JAXA Kyoto and Carbon project. He is also the Coprincipal Investigator of the German Aerospace Center Tandem-X mission. His current research interest includes continental-scale forest mapping with biomass indicators using high-resolution spaceborne SAR, wavelet multiresolution techniques for the approximation and analysis of SAR imagery, and the statistics of polarimetric-synthesized SAR images.



Alexandre Bouvet received the Engineering degree from the Ecole Nationale Supérieure d'Aéronautique et de l'Espace, Toulouse, France, in 2004 and the Ph.D. degree from Université Paul Sabatier-Toulouse III, Toulouse, in the Centre d'Etudes Spatiales de la Biosphère, in 2009. Since 2010, he has been a Postdoctoral Fellow with the European Commission Joint Research Center, Ispra, Italy, where he is working on the use of SAR data for the analysis of tropical forest cover dynamics. His interests include SAR image processing and the use of remote sensing data

to monitor vegetated areas for environmental applications.



Richard M. Lucas received the B.Sc. degree in biology and geography (first-class joint honors) and the Ph.D. degree, in the remote sensing of snow and vegetation using NOAA AVHRR and Landsat sensor data, from the University of Bristol, Bristol, U.K., in 1986 and 1989, respectively. He is currently a Professor with the Institute of Geography and Earth Sciences, Aberystwyth University, Aberystwyth, U.K., where he is involved primarily in the integration of single-date and timeseries SAR and optical (hyperspectral) and LiDAR data for retrieving the biomass

structure, and species/community composition of ecosystems ranging from subtropical woodlands to tropical forests and mangroves. His research is focused on the carbon dynamics and biodiversity of these systems and their response to natural and human-induced changes. He has authored or coauthored